

# Dual-beam symmetric illumination-observation TV holography system for measurements

**Nandigana Krishna Mohan**, MEMBER SPIE  
Indian Institute of Technology  
Department of Physics  
Applied Optics Laboratory  
Madras 600 036  
India

**Angelica Svanbro**, MEMBER SPIE  
**Mikael Sjödaahl**  
**Nils-Erik Molin**  
Luleå University of Technology  
Division of Experimental Mechanics  
S-971 87 Luleå  
Sweden  
E-mail: Angelica.Svanbro@mt.luth.se

**Abstract.** The Leendertz dual-beam symmetric illumination-normal observation arrangement is widely employed for real time evaluation of in-plane displacement components as well as surface shape. Instead of observing along the optical axis, we have examined the Leendertz arrangement by observing the scattered light along the direction of the illumination beams, and imaged it as two separate images onto the photo sensor of a CCD camera. The interferometer is a combination of two channels, each of which measures independently and simultaneously the information pertaining to either the in-plane displacement component of a deformation vector, or the surface relief variation of a three-dimensional object. In addition, a summary of possible measurements that can be carried out from the present arrangement is also highlighted. Experimental results using a four-frame phase shifting technique are illustrated. © 2001 Society of Photo-Optical Instrumentation Engineers. [DOI: 10.1117/1.1418010]

Subject terms: speckle interferometry; electronic/digital speckle pattern interferometry; TV holography; stereovision/stereoscopic systems; deformation measurement; shape measurement.

Paper 200415 received Oct. 24, 2000; revised manuscript received June 15, 2001; accepted for publication June 15, 2001.

## 1 Introduction

TV holography is a well established technique for measuring the deformation and surface shape of diffusely scattering objects.<sup>1-3</sup> A speckle correlation interferometer for measuring only an in-plane displacement component of a deformation vector was first suggested by Leendertz.<sup>4</sup> In this arrangement, two collimated beams symmetric with respect to the surface normal of a diffuse object are used for illumination, and the scattered fields generated are observed along the optical axis of the imaging lens. The interbeam angle between the two illuminating beams determines the sensitivity of the configuration. This arrangement is commonly employed for on-line evaluation of in-plane displacement components.<sup>5-7</sup> In addition, the Leendertz in-plane sensitive configuration is exploited to convert the in-plane motion of a curved specimen due to rotation of the object into depth variation of a 3-D object.<sup>8,9</sup> Recently a modification of the Leendertz method that leads to a twofold increase in the sensitivity has been proposed in the literature.<sup>10-13</sup> This is accomplished by observing the scattered fields independently along the direction of the illumination beams, combined at the observation plane. In the interferometer, for each illumination beam there are two scattered fields, that is, the back scattered field along the same direction of illumination and also the scattered field in the specular direction. Therefore, four beams interact at the observation plane. Hence, six phase terms are responsible for fringe formation, and the resultant interferogram obtained from this configuration contains the information pertaining to in-plane displacement with sensitivity proposed by Leendertz, as well as a twofold increase in sensitivity. For achieving twofold measuring sensitivity, the object is

coated with retroreflective paint to increase the light scattered back in the direction of the illumination beams, and also to suppress the contributions of the scattered light in the specular directions.<sup>11,12</sup> Krishna Mohan recently suggested a phase reversal technique<sup>13</sup> to completely eliminate the influence of cross interference terms in a twofold sensitivity configuration.

Instead of combining the four beams simultaneously at the observation plane, we have further examined and implemented for measurements the interferometer by independently imaging the scattered fields generated at the image plane, owing to dual beam symmetric illumination. The interferometer, also referred as the stereovision TV holography system, needs a single CCD camera for capturing and analyzing the two images simultaneously. A detailed theory of fringe formation, and the experimental results using a four-frame phase shifting technique on a circular aluminum plate and a cylindrical surface are presented.

## 2 Optical Arrangement

The optical arrangement is essentially two separate interferometers in which the scattered fields are observed along the direction of illuminating beams, and imaged as two separate images. The schematic diagram of the arrangement is shown in Fig. 1. The object is symmetrically illuminated with two collimated beams, making an angle  $\theta$  with respect to the symmetrical axis. The scattered fields are collected by means of a bimirror ( $M_1$  and  $M_2$ ) and a pair of beamsplitters ( $BS_1$  and  $BS_2$ ). The angle between the bimirror is fixed at 90 deg, while the beamsplitters are used for alignment. For each illumination beam there are two scattered fields: namely, the scattered field along the same direction

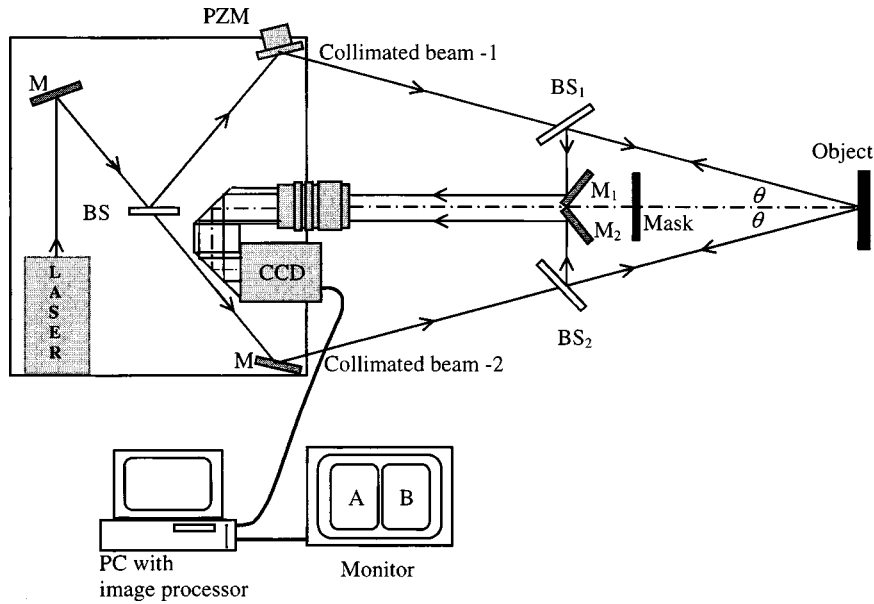


Fig. 1 Schematic arrangement of a dual-beam symmetric illumination-observation TV holography system.

of illumination (back scattered), and the scattered field in the symmetrically opposite direction (specular reflection direction). The scattered fields enter each half of a zoom video lens and relay lenses, and are imaged as two separate images (channel A and channel B) onto the CCD camera. The magnification of the imaging system is adjusted such that the two images occupy each half of the detector plane. A computer-controlled piezo electric driven mirror (PZM) is provided in the illumination beam-1 for introducing the phase steps in both the channels. The CCD and the PZM are connected to a commercially available image processing system that is interfaced to the host computer.<sup>14-16</sup>

### 3 Theory

In this stereovision arrangement, one half of the CCD camera detects the interference between the two speckle fields, which arises, from the illumination beam-1 along the same direction and the specular reflection speckle field from the illumination beam-2 (channel A), as shown in Fig. 2(a). Similarly, the second half of the detector array determines where the interference is between the back scattered field of the illumination beam-2 with the specular reflection field of

the illumination beam-1, along the direction of the illumination beam-2 (channel B) [Fig. 2(b)]. The intensity distribution recorded on the CCD camera, which represents the initial state of the object observed simultaneously along channels A and B, respectively, can be expressed as:<sup>16</sup>

$$I_{N(\text{channel A})} = I_1 + I_2 + 2\sqrt{I_1 I_2} \cos(\phi + \varphi_N), \quad (1)$$

$$I_{N(\text{channel B})} = I'_1 + I'_2 + 2\sqrt{I'_1 I'_2} \cos(\phi' + \varphi_N), \quad (2)$$

where  $(I_1, I_2)$  and  $(I'_1, I'_2)$  represent the intensities of the respective speckle fields generated in both the channels. The corresponding relative random phases are represented by  $\phi$  and  $\phi'$ , and  $\varphi_N$  represents the phase step values  $(0, \pi/2, \pi, 3\pi/2)$  introduced via the PZM provided in the illumination beam-1;  $N = 1, 2, 3, 4$ .

The object deformation causes a relative phase change in both the channels, and the final intensity distribution in each arm of the interferometer can now be written as:

$$I'_{N(\text{channel A})} = I_1 + I_2 + 2\sqrt{I_1 I_2} \cos(\phi + \Delta\phi_A + \varphi_N), \quad (3)$$

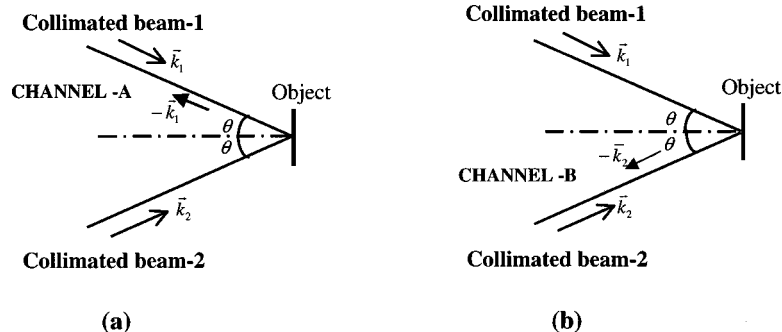


Fig. 2 Geometry of the illumination and observation propagation vectors in (a) channel A and (b) channel B for phase evaluation.

$$I'_{N(\text{channel B})} = I'_1 + I'_2 + 2\sqrt{I'_1 I'_2} \cos(\phi' + \Delta\phi_B + \varphi_N), \quad (4)$$

where  $\Delta\phi_A = \Delta\phi_1 - \Delta\phi_2$  and  $\Delta\phi_B = \Delta\phi_3 - \Delta\phi_4$  are the relative phase changes introduced in channels A and B due to the deformation field.

Two sets of four phase-shifted images stored before the deformation, together with those stored after, are used to generate correlation fringe patterns. Operating the system in display mode, interference patterns are observed at video rate speed, and are modulated by cosinusoidal function of the form<sup>16</sup>:

$$I_{(\text{channel A})} = \left| 8\sqrt{I_1 I_2} \cos\left[\frac{\Delta\phi_A}{2}\right] \right|^2 \quad (5)$$

$$I_{(\text{channel B})} = \left| 8\sqrt{I'_1 I'_2} \cos\left[\frac{\Delta\phi_B}{2}\right] \right|^2. \quad (6)$$

### 3.1 Measurement of In-Plane Displacement and Shape

The phase terms  $(\Delta\phi_1, \Delta\phi_2)$  in channel A and  $(\Delta\phi_3, \Delta\phi_4)$  in channel B responsible for fringe formation can be illustrated by viewing in the directions of the illumination and observation beams (Fig. 2). The phase terms are related to the displacement vector  $\vec{L}$  through the following expressions<sup>12,13</sup>

Channel A

$$\begin{aligned} \Delta\phi_1 &= (-\vec{k}_1 - \vec{k}_1) \cdot \vec{L} \\ \Delta\phi_2 &= (-\vec{k}_2 - \vec{k}_1) \cdot \vec{L} \end{aligned} \quad (7)$$

Channel B

$$\begin{aligned} \Delta\phi_3 &= (-\vec{k}_2 - \vec{k}_1) \cdot \vec{L} \\ \Delta\phi_4 &= (-\vec{k}_2 - \vec{k}_2) \cdot \vec{L}, \end{aligned} \quad (8)$$

where  $\vec{k}_1$  and  $\vec{k}_2$  are the dual-beam symmetric illumination propagation vectors as shown in Fig. 2. The relative phase changes  $\Delta\phi_A$  and  $\Delta\phi_B$  can be derived from Eqs. (7) and (8) as:

$$\Delta\phi_A = \Delta\phi_1 - \Delta\phi_2 = (\vec{k}_2 - \vec{k}_1) \cdot \vec{L}, \quad (9)$$

$$\Delta\phi_B = \Delta\phi_3 - \Delta\phi_4 = (\vec{k}_2 - \vec{k}_1) \cdot \vec{L}. \quad (10)$$

Assuming that the illuminating beams with an interbeam angle of  $2\theta$  are confined to the  $x$ - $z$  plane, then

$$\Delta\phi_A = \Delta\phi_B = \frac{4\pi}{\lambda} u \sin\theta. \quad (11)$$

Here the propagation vectors  $\vec{k}_1 = 2\pi(-\hat{i} \sin\theta - \hat{k} \cos\theta)/\lambda$ ,  $\vec{k}_2 = 2\pi(\hat{i} \sin\theta - \hat{k} \cos\theta)/\lambda$  and the displacement vectors  $\vec{L} = \hat{i}u + \hat{j}v + \hat{k}w$  have been used.

Equation (11) shows that two sets of correlation fringe patterns observed on the monitor contain information per-

taining to the in-plane displacement component ( $u$ ) of the deformation vector with identical measuring sensitivities. The sensitivity is the same as reported in the Leendertz method.

The optical arrangement can also be implemented for shape evaluation. The concept of contouring is based on the fact that for very small angles of rotation (tilt), points at the same depth along the viewing direction undergo equal in-plane displacements, and this displacement is directly proportional to the depth of those points. Considering that the object rotation is  $\Delta\xi$ , we obtain a relation between the relative phase changes in channels A and B and the height of the three-dimensional surface as<sup>8,9</sup>:

$$\Delta\phi_A = \Delta\phi_B = \frac{4\pi}{\lambda} z \sin\Delta\xi \sin\theta. \quad (12)$$

The phase variation terms in Eq. (12) clearly indicate that the interferograms obtained from channels A and B contain information related to the height variation profile of the 3-D surface with identical measuring sensitivities. Even though the measuring sensitivities are the same in channels A and B, the section of the 3-D object under observation is different due to off-axis symmetrical viewing. The arrangement therefore simultaneously permits the study of different sectional views of a 3-D object. In stitching the two views together, one realizes that the spatial sampling ( $x, y$  coordinates) is somewhat different in the two views. The spatial sampling (expressed in global object coordinates) will depend on the angle between the local normal vector of the object surface and the orientation of the detector, as seen from each of the views. Since the observation directions coincide with the two illumination directions, the spatial sampling rate will in general be different in the two images. The difference in the spatial sampling rate may ultimately result in a loss of details in one of the views that are resolved in the other.

The optical arrangement can be modified and implemented for other applications. A summary of possible measurements that can be carried out from the proposed configuration is shown in Table 1. As stated in the introduction, the arrangement shown in Table 1 part B yields twofold measuring sensitivity for the in-plane displacement component when the contributions of cross-interference terms owing to four beam interaction at the observation plane are suppressed.<sup>11-13</sup> The interference between the phase terms  $\Delta\phi_1$  and  $\Delta\phi_4$ , which corresponds to the waves that are scattered back along the direction of illumination beams, results in a twofold increase in sensitivity.

### 3.2 Measurement of Out-of-Plane Displacement

Part C in Table 1 represents an arrangement for sensing the out-of-plane displacement component of a deformation vector. The object is illuminated by a collimated beam at an angle  $\theta$ , defined by the propagation vector  $\vec{k}_1$ . The observation direction is symmetrically opposite to the illumination beam (i.e., along the specular reflection direction; observation vector  $\vec{k}_2$ ). The scattered light is collected by means of mirrors  $M_1$  and  $M_2$  and imaged onto the CCD camera via an imaging element (L). A smooth reference wave derived from the same laser source is added with the

**Table 1** Optical arrangement and the corresponding data that can be extracted.

Fig. No.	Optical Arrangement	Fringe Formation Equations	
		In terms of Propagation vectors	In terms of Physical parameters
A		$\Delta\phi_A = (\vec{k}_2 - \vec{k}_1) \cdot \vec{L}$ $\Delta\phi_B = (\vec{k}_2 - \vec{k}_1) \cdot \vec{L}$	<p><u>In-plane displacement</u></p> $\Delta\phi_A = \frac{4\pi}{\lambda} u \sin \theta$ $\Delta\phi_B = \frac{4\pi}{\lambda} u \sin \theta$ <p><u>Shape</u></p> $\Delta\phi_A = \frac{4\pi}{\lambda} z \sin \Delta\xi \sin \theta$ $\Delta\phi_B = \frac{4\pi}{\lambda} z \sin \Delta\xi \sin \theta$
B		$\Delta\phi_{AB} = 2(\vec{k}_2 - \vec{k}_1) \cdot \vec{L}$	<p><u>In-plane displacement</u></p> $\Delta\phi_{AB} = \frac{8\pi}{\lambda} u \sin \theta$
C		$\Delta\phi = (\vec{k}_2 - \vec{k}_1) \cdot \vec{L}$	<p><u>Out-of-plane displacement</u></p> $\Delta\phi = \frac{4\pi}{\lambda} w \cos \theta$
D		$\Delta\phi_A = (\vec{k}_2 - \vec{k}_1) \cdot \vec{L}$ $\Delta\phi_B = -(\vec{k}_2 + \vec{k}_1) \cdot \vec{L}$	<p><u>Displacement</u></p> $\Delta\phi_A = \frac{4\pi}{\lambda} u \sin \theta$ $\Delta\phi_B = \frac{4\pi}{\lambda} w \cos \theta$ <p><u>Shape</u></p> $\Delta\phi_A = \frac{4\pi}{\lambda} z \sin \Delta\xi \sin \theta$ $\Delta\phi_B = \frac{4\pi}{\lambda} x \sin \Delta\xi \cos \theta$

help of a single mode fiber and a beamsplitter, BS, to the image.<sup>17,18</sup> The phase change that can be expressed in terms of direction of illumination ( $\vec{k}_1$ ), and observation ( $\vec{k}_2$ ) is defined in Table 1. The measuring sensitivity can be varied by changing the illumination-observation angle,  $\theta$ , with respect to the optical axis. Increasing the illumination-observation angle in the arrangement allows the measurement of large-object deformation with reduced sensitivity, which is an important requirement in nondestructive evaluation.<sup>19,20</sup>

### 3.3 Measurement of Both In-Plane and Out-of-Plane Displacement

An optical configuration by combining Part A in Table 1 (Fig. 1) and Part C into one single arrangement for parallel evaluation of the in-plane ( $u$ ) and out-of-plane ( $w$ ) displacement components of a deformation vector is shown in Part D in Table 1. In this arrangement, the object is illuminated symmetrically with two collimated beams, and the scattered fields are observed along the direction of one of the illumination beams (channel A) for measuring the in-plane displacement ( $u$ ).

The scattered field from the same illuminated beam in the specular direction is combined with a smooth reference beam (channel B) for parallel evaluation of the out-of-plane displacement ( $w$ ).<sup>21</sup> Mechanical shutters  $S_1$ ,  $S_2$ , and  $S_3$  are introduced in the path of the illumination-observation beams to incorporate a four-exposure method, by operating the image processor in a time-lapse save mode. The time-lapse mode permits the saving of a series of static holograms of an object and generates either cosine fringes or wrapped phase maps in a controlled manner.

In the parallel evaluation method, the first exposure that represents the initial state of the object observed from channel A is stored in the image processor by closing the shutter  $S_1$ . Blocking the illumination beam-2 allows the recording of the interference between the back scattered field along the direction of illumination beam-1 with the scattered field in the same direction, because of the specular reflection of the illumination beam-2. Similarly, the second exposure that represents the initial state of the object from channel B is recorded by opening the shutter  $S_1$ , and closing the shut-

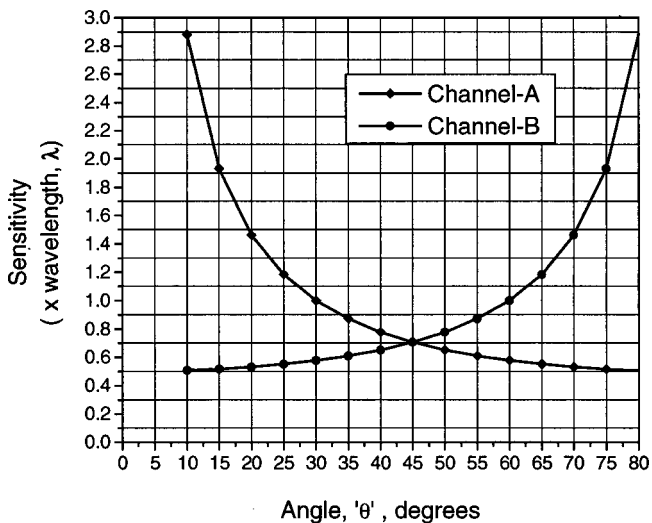


**Fig. 3** Theoretical profile of sensitivity variation with respect to the illumination-observation beam angle,  $\theta$ , in channels A and B, respectively. The measuring sensitivities are identical in both the configurations when  $\theta = 45$  deg.

ters  $S_2$  and  $S_3$ . This allows only the recording of the interference between the scattered field in the specular direction from the illumination beam-1 with a smooth reference beam. The object deformation causes a path length change in channels A and B, and the subsequent exposures 3 and 4, under similar observation conditions described earlier, are stored in the processor. A set of four phase-shifted images stored in the image processor from exposure 1 are used together with the set of images stored from exposure 3 to generate correlation fringes corresponding to in-plane displacement from channel A. Similarly, a set of images from exposure 2 used together with a set of images from exposure 4 yields out-of-plane displacement.

Equations for the fringe formations derived are shown in Table 1. The phase variation terms,  $\Delta\phi_A$  and  $\Delta\phi_B$ , (Table 1) clearly indicate that the measuring sensitivities in both the channels are dependent on an oblique illumination-observation beam angle,  $\theta$ , the angle to the symmetrical axis. When  $\theta$  is increasing, the distance between the two adjacent contour planes in the fringe pattern generated in channel A keeps reducing, while in channel B the correlation fringes will be broadening further. This phenomenon can be observed from the theoretical plot shown in Fig. 3. It is interesting to note that both the components can be

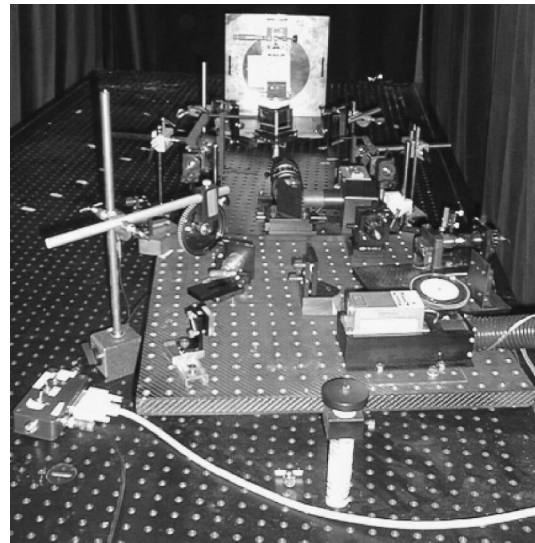


**Fig. 4** The optical head of a stereovision TV holography system.

sensed from the setup with identical measuring sensitivities when the illumination-observation angle,  $\theta$  is 45 deg (i.e.,  $0.707\lambda$ ). Hence, the method provides a scope for trade-off between the in-plane and out-of-plane measuring sensitivity.

#### 4 Experimental Results

The experiments are conducted on an aluminum plate ( $110 \times 75 \times 1$  mm<sup>3</sup>) and a cylindrical surface. The specimens are coated with matt white spray paint. Two collimated illumination beams, with 40 mm diam from a frequency-doubled diode-pumped 80-mW laser ( $\lambda = 532$  nm), symmetric to surface normal, illuminate the object. To receive the scattered fields in the directions of the illumination beams, two beamsplitters having a transmission and reflection ratio of approximately 50:50 coating at 532 nm, and a fabricated bimirror are used in the experimental setup. The scattered fields are collected and imaged onto a NEC TI-324A CCD camera via a combination of zoom video lens and relay lenses. The magnification of the imaging system is adjusted such that the two images as separate images (A and B) occupy each half of the detector plane. A computer-controlled PZM is provided in the illumination beam-1, as shown in Fig. 1. A photograph that

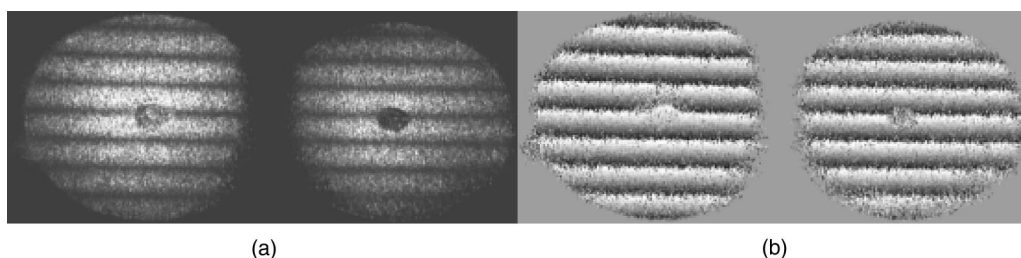


**Fig. 5** Interferograms and corresponding phase maps obtained simultaneously from channels A and B for an aluminum plate subjected to rotation in its own plane. The illumination-observation angle is  $\theta \sim 20$  deg.

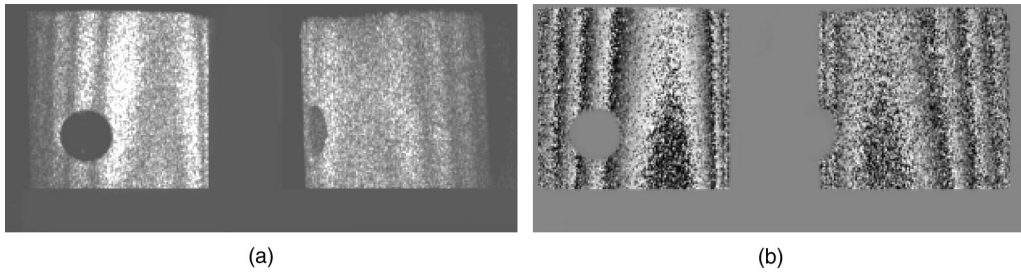


**Fig. 6** Interferograms and corresponding phase maps obtained simultaneously from channels A and B for a cylindrical surface subjected to rotation around the  $y$  axis. The illumination-observation angle is  $\theta \sim 40$  deg.

represents the general view of the optical head developed at Luleå University of Technology and implemented in the present experiments is shown in Fig. 4.

In the first experiment, the aluminum plate is subjected to rotation in its own plane, and the real time  $u$ -component of in-plane correlation fringes recorded directly from the monitor is shown in Fig. 5(a). It can be seen from the photograph that the fringe patterns are identical and the contrast of the fringes obtained from both the channels are quite good. The fringe spacing ( $\Delta u = \lambda/2 \sin \theta$ ) is equal to 778 nm. Figure 5(b) represents the corresponding evaluated phase maps.

In the second experiment, a cylindrical surface is subjected to rotation around the  $y$  axis (vertical axis). The real-time contour fringe patterns generated from both the channels seen on the TV monitor, and the corresponding phase maps are shown in Figs. 6(a) and 6(b), respectively. The present study clearly shows that one can record and analyze different sectional views of 3-D objects. Remember, however, that the spatial sampling is different in the two views, a fact manifested by the difference in interfringe distance between corresponding fringes in the two views in Fig. (6) when the surface normal differs from the axis of symmetry. For a true shape measurement, therefore, the two views have to be transformed from the coordinate systems of the detector into the global object coordinate system. The dual-beam symmetric illumination-observation arrangement is

similar to existing stereovision systems,<sup>22,23</sup> and in comparison, the present setup had a distant advantage; that is, it needs a single imaging system for simultaneous observation and analysis.

An optical configuration shown in Part D in Table 1 is also examined experimentally for parallel evaluation of displacement components on a cylindrical surface. Following the procedure of sequentially blocking the beams with the help of mechanical shutters, between the four exposures (as explained earlier in Sec. 3), the extracted in-plane motion of the object that represents the surface variation of a cylindrical surface obtained from channel A is shown respectively in Figs. 7(a) and 7(b), in terms of phase map and 3-D surface profile (where the  $i$  and  $j$  axes are detector coordinates). Similarly, the phase and 3-D maps, because of the rotation of the specimen, evaluated from channel B are shown in Figs. 8(a) and 8(b), respectively. The experimental results show good agreement with the theoretical predictions. The results demonstrated with phase stepping indicate the use of the proposed method as an alternative tool for measuring the two sensitivity vectors of a deformation vector for 2-D as well as 3-D objects.

## 5 Conclusions

We report an optical arrangement based on the Leendertz dual-beam illumination configuration for displacement and

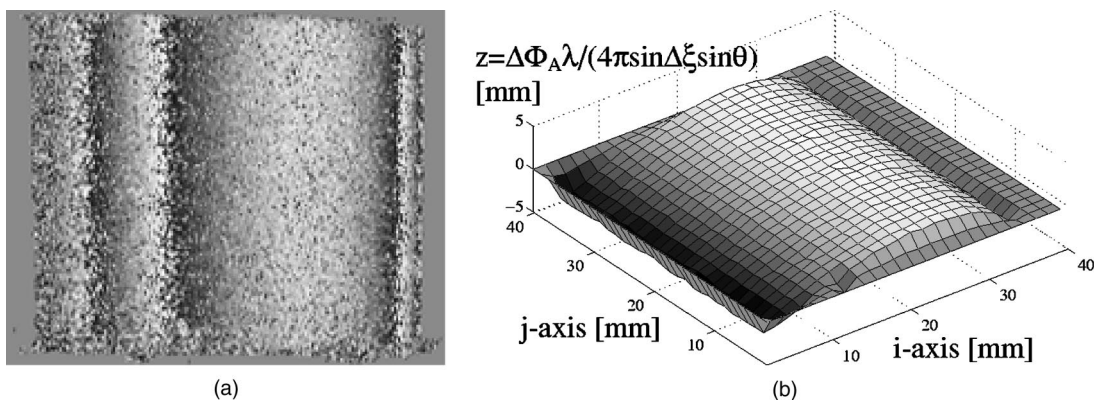


**Fig. 7** Channel A: (a) phase map and (b) 3-D surface profile. The results are obtained for a cylindrical surface subjected to rotation around the  $y$  axis from an in-plane sensitive configuration. The illumination-observation angle is  $\theta \sim 40$  deg. The results are extracted by using together a set of phase-shifted images stored in the image processor from exposure 1 with a set of phase-shifted images from exposure 3.

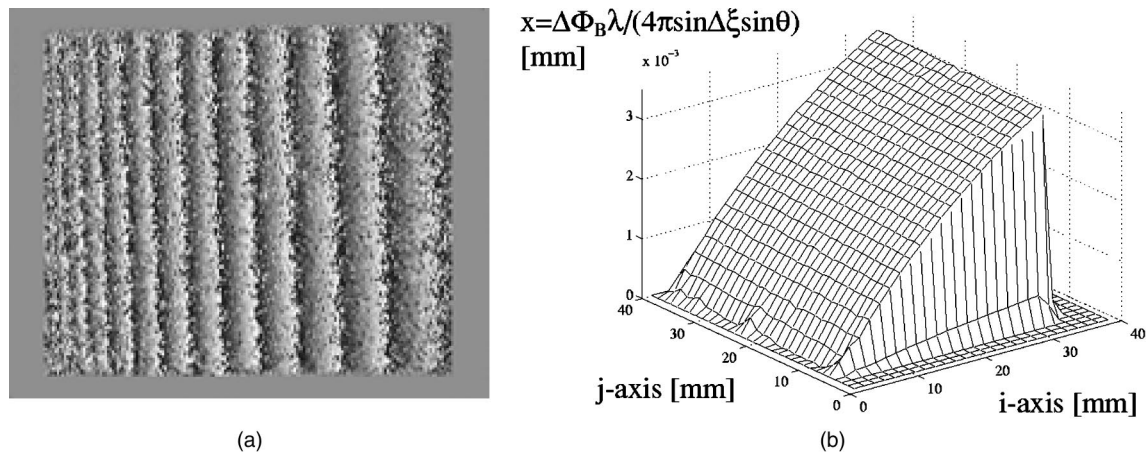


**Fig. 8** Channel B: (a) phase map and (b) 3-D surface profile. The results are obtained for a cylindrical surface subjected to rotation around the  $y$  axis from an out-of-plane sensitive configuration. The illumination-observation angle is  $\theta \sim 40$  deg. The results are extracted by using together a set of phase-shifted images stored in the image processor from exposure 2 with a set of phase-shifted images from exposure 4.

shape measurements. A summary of the possible measurements that can be carried out from the arrangement is illustrated with experimental support. The proposed method of dual-beam symmetric illumination-observation arrangement may find useful applications in other areas of engineering metrology.

#### Acknowledgments

The experiments were performed at Luleå University of Technology when Dr. Krishna Mohan was a visiting scientist at the Laboratory in May through June 1999 under a joint collaborative research program. The Swedish Foundation for Strategic Research-Integral Vehicle Structures (SSF/IVS) research program in Sweden, and the Swedish Research Council for Engineering Sciences (TFR) support this project.

#### References

- O. J. L okberg, "Recent developments in video speckle interferometry," Chap. 4 in *Speckle Metrology*, R. S. Sirohi, Ed., pp. 157–194, Marcel Dekker Inc., New York (1993).
- C. Joenathan, "Speckle photography, shearography and ESPI," Chap. 6 in *Optical Measurement Techniques and Applications*, P. K. Rastogi, Ed., pp. 151–182, Artech House, Boston, MA (1997).
- R. P. Tatam, "Optoelectronic developments in speckle interferometry," *Proc. SPIE* **2860**, 194–212 (1996).
- J. A. Leendertz, "Interferometric displacement measurement on scattered surface utilizing speckle effects," *J. Phys. E* **3**, 214–218 (1970).
- R. Jones, "The design and application of a speckle pattern interferometer for total plane strain field measurement," *Opt. Laser Technol.* **8**, 215–219 (1976).
- C. S. Vikram and M. J. Pechersky, "Wedge prism for direction resolved speckle correlation interferometry," *Opt. Eng.* **38**(10), 1743–1747 (1999).
- B. Bowe, S. Martin, V. Toal, A. Langhoff, and M. Whelan, "Dual in-plane electronic speckle pattern interferometry system with electro-optical switching and phase shifting," *Appl. Opt.* **38**, 666–673 (1999).
- A. R. Ganesan and R. S. Sirohi, "A new method of contouring using digital speckle pattern interferometry (DSPI)," *Proc. SPIE* **954**, 327–332 (1988).
- C. Joenathan, B. Pfister, and H. J. Tiziani, "Contouring by electronic speckle pattern interferometry employing dual beam illumination," *Appl. Opt.* **29**, 1905–1911 (1990).
- R. S. Sirohi and N. Krishna Mohan, "In-plane displacement measurement configuration with twofold sensitivity," *Appl. Opt.* **32**, 6387–6390 (1993).
- A. Sohmer and C. Joenathan, "Twofold increase in sensitivity with a dual beam illumination arrangement for electronic speckle pattern interferometry," *Opt. Eng.* **35**(7), 1943–1948 (1996).
- T. Santhanakrishnan, P. K. Palanisamy, and R. S. Sirohi, "Fringe formation in an in-plane displacement measurement configuration with twofold increase in sensitivity: theory and experiment," *Appl. Opt.* **37**, 4150–4153 (1998).
- N. Krishna Mohan, "Measurement of in-plane displacement with twofold sensitivity using phase reversal technique," *Opt. Eng.* **38**(12), 1964–1966 (1999).
- K. A. Stetson, W. R. Brohinsky, J. Wahid, and T. Bushman, "An electro-optic holography system with real-time arithmetic processing," *J. Nondestruct. Eval.* **8**, 69–76 (1989).
- K. A. Stetson, "Electro-optic holography system for vibration analysis and non destructive testing," *Opt. Eng.* **26**(12), 1234–1239 (1987).
- R. J. Pryputniewicz, "Electro-optic holography," Chap. 3 in *Holographic Interferometry—Principles and Methods*, P. K. Rastogi, Ed., pp. 59–74, Springer-Verlag, Berlin (1994).
- N. Krishna Mohan, H. O. Saldner, and N.-E. Molin, "Electronic speckle pattern interferometry for simultaneous measurement of out-of-plane displacement and slope," *Opt. Lett.* **18**, 1861–1863 (1993).
- H. O. Saldner, N. Krishna Mohan, and N.-E. Molin, "Comparative TV holography for vibration analysis," *Opt. Eng.* **34**(2), 486–492 (1995).
- E. Vikhagen, "Non destructive testing by use of TV holography and deformation phase gradient calculation," *Appl. Opt.* **29**, 137–144 (1990).
- J. T. Malmo and O. J. L okberg, "Detection of defects in composite materials by TV holography," *NDT Intl.* **21**, 223–228 (1988).
- N. Krishna Mohan, A. Andersson, M. Sj odahl, and N.-E. Molin, "Optical configuration for TV holography measurement of in-plane and out-of-plane deformations," *Appl. Opt.* **39**, 573–577 (2000).
- M. A. Sutton, Y. J. Chao, and P. F. Luo, "Application of stereovision in three-dimensional deformation analysis in fracture experiments," *Opt. Eng.* **33**(3), 981–999 (1994).
- P. Synnergren, "Measurement of three dimensional displacement fields and shape using electronic speckle photography," *Opt. Eng.* **36**(8), 2302–2310 (1997).



**Nandigana Krishna Mohan** received his MSc(Tech) degree in applied physics from Andhra University, Waltair, and his MS (Eng) and PhD degree in mechanical engineering from the Indian Institute of Technology (IIT), Madras. Currently he is working as a Technical Officer (Selection Grade) at IIT. He worked as a visiting scientist at Universit at Oldenburg, Germany in 1991 under an INSA-DFG fellowship program, and as a visiting scientist at Lule  University of Technology, Sweden, in 1993, 1995, and 1999. He was

also an associate research officer for the National Research Council, Ottawa, Canada, in 1997. His research areas include holographic/speckle and speckle shear interferometry, TV holography and shearography, digital speckle photography, stereovision systems, and optical metrology using photorefractive materials. His present on-going research projects are a Doppler Michelson Interferometer for measuring in-bore velocity time history of a projectile, phase reversal technique for image subtraction and optical metrology; and multichannel two wave mixing in PR crystals for data storage. He is also a program committee member for various conferences. He has published and presented approximately 82 papers in these research areas. He is member of SPIE and a life member of the Optical Society of India.



**Angelica Svanbro** (née Andersson) obtained her MSc in engineering physics from Luleå University of Technology, Sweden, in 1998. Since then she has been a PhD student at the division of Experimental Mechanics at Luleå University of Technology. Her research field is speckle metrology.



**Mikael Sjö Dahl** received his MS in mechanical engineering and his PhD in experimental mechanics from the Luleå University of Technology, Sweden, in 1989 and 1995, respectively. He is currently an associate professor at the division of Experimental Mechanics at the Luleå University of Technology. He has authored or coauthored approximately 30 papers in international journals and contributed to two books. His research interests include digital speckle metrology, experimental stress analysis, and digital image processing.



**Nils-Erik Molin** received his PhD in 1970 at Physics II, Royal Institute of Technology, Stockholm, Sweden. From 1971 to 1988 he was a senior lecturer and thereafter professor in experimental mechanics at Luleå University of Technology, Sweden. His research field is optical metrology.